Photoinduced linkage isomerism of binuclear bis(pyrazole-3,5-dicarboxylato)-bridged {RuNO}^{6} centres

Anna Zangl [a], Peter Klüfers [a,*], Dominik Schaniel [b], Theo Woike [b]

[a] *Department für Chemie und Biochemie, Ludwig-Maximilians-Universität, Butenandtstraße 5–13, 81377 München, Germany*
[b] *I. Physikalisches Institut, Universität zu Köln, Zülpicherstraße 77, 50937 Köln, Germany*

A R T I C L E   I N F O

A B S T R A C T

The two novel binuclear pyrazole-3,5-dicarboxylato-bridged {RuNO}^{6} complexes $K_2[\{Ru(NO)Cl\}_2(\mu\text{-pzdc})_2]$ (**1**) and $[\{Ru(NO)(H_2O)\}_2(\mu\text{-pzdc})_2]\cdot 4H_2O$ (**2**) (pzdc = pyrazole-3,5-dicarboxylate) were synthesized and characterized by elemental analysis, mass spectrometry and spectroscopic methods (NMR, UV–vis, IR). **2** was investigated by means of single-crystal X-ray diffraction analysis. On irradiation, in both **1** and **2** the existence of photoinduced long-lived metastable isonitrosyl states SI were detected by low-temperature infrared spectroscopy.

© 2009 Elsevier B.V. All rights reserved.

Mononuclear ruthenium nitrosyl compounds, but also a few ruthenium nitrosyls of higher nuclearity, have been investigated as potential candidates for NO delivery upon light irradiation in photodynamic therapy (PDT). Photoinduced linkage isomerism (PLI) is an alternative way for a Ru(NO) moiety to consume excitation energy in the visual range. The photoinduced formation of nitrosyl linkage isomers may be an early step in the pathways used for PDT [1]. In the course of the PLI process, the nitrosyl ligand can be switched by light into two metastable isomeric configurations. Thereby, the linear κN-bonded configuration M–N–O of the ground-state (GS) can be transferred to the linear κO-bonded isonitrosyl configuration M–O–N (MS1) and the $\kappa N,O$ side-on-bonded configuration (MS2). PLI is well documented for mononuclear nitrosyl complexes with various central atoms (Fe, Ru, Os, Mn, Ni, Pt, Re) and ligands (F^-, Cl^-, Br^-, I^-, CN^-, NH_3, NO_2^-, pyridine), almost arbitrary counter ions and other constituents of the solids such as crystal water [2]. Herein we show that the PLI of NO is also possible for binuclear complexes. The examples presented are the chlorido-ruthenate $K_2[\{Ru(NO)Cl\}_2(\mu\text{-pzdc})_2]$ (**1**) and the analogous electroneutral aqua complex $[\{Ru(NO)(H_2O)\}_2(\mu\text{-pzdc})_2]\cdot 4H_2O$ (**2**) which are both of the {RuNO}^{6} type [3].

Using the starting materials $K_2[Ru(NO)Cl_5]$ and pyrazole-3,5-dicarboxylic acid (pzdcH$_3$), the binuclear chlorido-ruthenate $K_2[\{Ru(NO)Cl\}_2(\mu\text{-pzdc})_2]$ (**1**) was obtained as an amorphous yellow powder [4,5]. In an aqueous solution of **1**, ligand exchange took place, resulting in the formation of the aqua complex $[\{Ru(NO)(H_2O)\}_2(\mu\text{-pzdc})_2]$. The latter formed yellow crystals of the tetrahydrate $[\{Ru(NO)(H_2O)\}_2(\mu\text{-pzdc})_2]\cdot 4H_2O$ (**2**) [4,6]. The molecular structure in crystals of **2** is depicted in Fig. 1, together with the most significant bond distances and angles, a puckering analysis, hydrogen bonds and short intermolecular non-hydrogen contacts [7]. The asymmetric unit (space group $P\bar{1}$) contains two molecules of crystal water and one half of the binuclear, centrosymmetric complex molecule. The electroneutral $[\{Ru(NO)(H_2O)\}_2(\mu\text{-pzdc})_2]$ molecules are made up of two {RuNO}^{6} fragments which are coordinated by two trianionic and tetradentate pzdc ligands. The symmetrically equivalent ruthenium centres are in a distorted octahedral environment with the nitrosyl and the aqua ligands defining molecular axes. The equatorial plane contains two *cis*-nitrogen and two *cis*-oxygen atoms about each central metal atom. All atoms of the pzdc ligands are roughly part of the plane spanned by the equatorial positions leading to an approximate C_{2h} symmetry of the binuclear compound. The O91–Ru1–N1 and Ru1–N1–O1 angles of the molecular axis are close to 180°. All equatorial ligand atoms (L_{eq}) adopt L_{eq}– Ru1–N1 angles larger than 90° and are therefore tilted away from the nitrosyl group. The almost planar five-membered chelate rings are only slightly puckered as is the six-membered central ring Ru1–N2–N3^i–Ru1^i–N2^i–N3. The crystal structure of **2** exhibits a distinct hydrogen-bond system.

Irradiation of **1** and **2** in the spectral range from 442 to 514 nm at temperatures below 200 K led to the formation of the Ru–O–N (MS1) isomer, which was identified by the shift of the v(NO) vibration to lower wavenumbers [9,10]. As shown in Fig. 2, in both **1** and **2** the area of the v(NO) ground-state vibration decreased upon illumination while new bands arose at lower wavenumbers. In **1** the threefold split GS-v(NO) band shifted from 1927/1905/1881 cm^{-1}
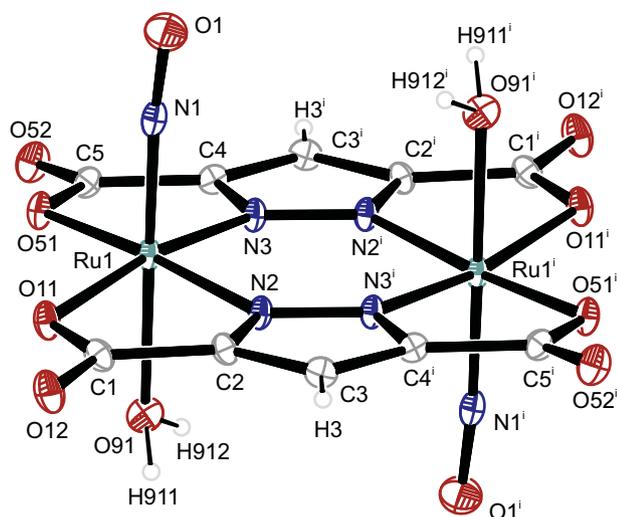
Fig. 1. The molecular structure of the binuclear complex in crystals of [{Ru(NO)-(H₂O)}₂(μ-pzdc)₂]·4H₂O (**2**) (50% probability ellipsoids). Interatomic distances [Å] and angles [°] (standard deviations in parentheses): from Ru1 to: O11 2.103(2), O51 2.096(2), O91 2.033(2), N1 1.744(2), N2 1.992(2), N3 1.984(2); N1–O1 1.140(3); O11–Ru1–N1 93.93(9), O11–Ru1–N2 75.97(8), O51–Ru1–N1 95.18(9), O51–Ru1–N3 76.46(8), O91–Ru1–N1 178.57(9), N1–Ru1–N3 93.32(9), N2–Ru1–N3 99.84(8), Ru1–N1–O1 174.5(2). Puckering analysis [8]: Ru1–O11–C1–C2–N2: $Q_2 = 0.094(2)$ Å; Ru1–N2–N3^i–Ru1^i–N2^i–N3: $Q = 0.078(2)$ Å. Donor–acceptor distances in hydrogen bonds [Å]: O91···O92^{ii} 2.489(3), O91···O52^{iii} 2.631(3), O92···O12 2.778(3), O92···O93^{iv} 2.696(3), O93···O12 2.809(3), O93···O11^v 2.780(3). Symmetry codes: ^{i}1 − x, −y, −z; ^{ii}1 − x, −y, 1 − z; ^{iii}−x, −y, −z.
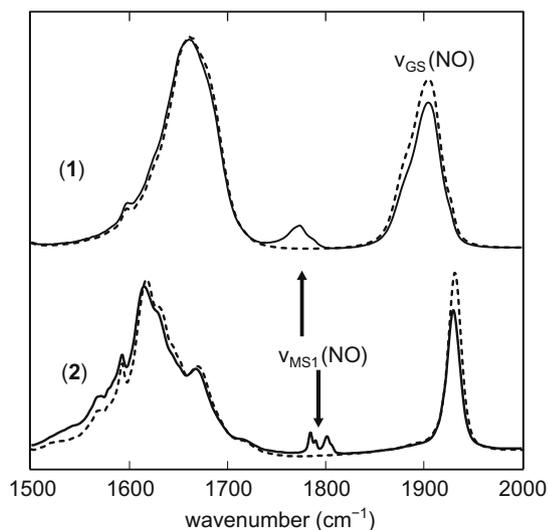

Fig. 2. Infrared spectra of **1** (top) and **2** (bottom) before (dashed) and after (solid) irradiation with light of $\lambda = 476$ nm at $T = 80$ K in the range of 1500–2000 cm^{-1}. Ordinate: extinction in arbitrary units; spectra vertically shifted.

to 1777/1774/1765 cm^{-1} by 150, 131, and 116 cm^{-1}, respectively, while in **2** the single GS-v(NO) band at 1932 cm^{-1} was split into four bands in MS1 and shifted to 1806, 1801, 1790, and 1775 cm^{-1}. From the decrease of the GS band the population of the isomeric configuration was determined under the assumption that no NO release occurred during illumination. We obtained 18.6% population for MS1 in **1** and 20.7% for MS1 in **2**. After saturation of the isomeric configuration, no further changes in the infrared spectrum were observed. The ground-state was fully recovered by illumination with light of 660 nm [11] or by heating to room temperature. Thus we conclude that no measurable NO

release occurred during illumination which would have biased the population calculation. The maximal population of MS1 was obtained with 476 nm excitation wavelength for **1** and 458 nm for **2**. After irradiation with light in the green or violet spectral range, the population of MS1 decreased.

In **1** we found the splitting of the NO vibration in three bands (a central excitation and two shoulders) both in the GS and MS1. In **2** the splitting into four bands (two groups of two bands) was only observed for the MS1 state. The origin of the splitting is assumed to be in the local surroundings of the isonitrosyl ligand in the crystal structure of **2** where the Ru–O–N moiety finds itself embedded in a hydrogen-bonded assembly of water molecules and a carboxylate function of adjacent molecules. Whether or not the binuclear nature of the complex contributes to the splitting will be investigated in future work. The change in area and position from 1618 cm^{-1} to 1615 cm^{-1} in **2** may be due to the influence of the isonitrosyl ligand on the deformation mode of the aqua ligand *trans* to it.

The second PLI isomer, the side-on MS2 configuration, was not identified directly by IR spectroscopy due to the presence of strong δ(H₂O) and CO/CN bands in the spectral region of 1700–1500 cm^{-1}, where one expects the stretching vibration of NO in MS2 [9]. However, after illumination of the MS1 state with 1064-nm radiation, which normally induces the transfer of MS1 to MS2 [11], the MS1-v(NO) band vanished while the GS-v(NO) band was not fully recovered. Only by subsequent illumination with 660 nm was the GS-v(NO) band fully recovered. This behaviour is a strong indication for the presence of MS2 after the transfer with 1064 nm, as known, for example, from nitrosyl complexes embedded in silica xerogels where the MS2-v(NO) band is hidden by the strong absorption bands of the silica matrix [12].

In conclusion, two binuclear {RuNO}^{6}-type complexes with linear Ru–N–O fragments and bridging tetradentate pzdc ligands were synthesised and characterised. Low-temperature infrared spectroscopy after irradiation with light in the spectral range of 442–514 nm showed that both compounds are capable of PLI as to the NO ligand. The metastable κO-bonded isonitrosyl MS1 state was generated from the κN-bonded nitrosyl GS states and reached populations of up to about 20%. The investigation of the κN, O side-on-bonded MS2 states was hampered by the superposition of various bands in the relevant frequency range of the infrared spectrum. However, the generation of MS2 in **1** und **2** was assumed by reason of the still-decreased GS band area after irradiation of the saturated MS1 state with 1064 nm.

Acknowledgements

Appendix A. Supplementary material

CCDC 728661 contains the supplementary crystallographic data for (**2**). These data can be obtained free of charge from the Cambridge Crystallographic Data Centre via www.ccdc.cam.ac.uk/data_request/cif. Supplementary data associated with this article can be found, in the online version, at doi:10.1016/j.inoche.2009.08.021.

References

[1] (a) M.J. Rose, P.K. Mascharak, Coordn. Chem. Rev. 252 (2008) 2093;
(b) M. Videla, S.E. Braslavsky, J.A. Olabe, Photochem. Photobiol. Sci. 4 (2005) 75.
[2] (a) T.E. Bitterwolf, Coordn. Chem. Rev. 250 (2006) 1196;
(b) P. Coppens, I. Novozhilova, A. Kovalevsky, Chem. Rev. 102 (2002) 861;
(c) P. Gütlich, Y. Garcia, Th. Woike, Coordn. Chem. Rev. 219–221 (2001) 839;

(d) H. Zöllner, W. Krasser, Th. Woike, Chem. Phys. Lett. 161 (1989) 497;

(e) K. Ookubo, Y. Morioka, H. Tomizawa, E. Miki, J. Mol. Struct. 379 (1996) 241;

(f) D. Schaniel, Th. Woike, B. Delley, D. Biner, K.W. Krämer, H.-U. Güdel, Phys. Chem. Chem. Phys. 9 (2007) 5149;

(g) D. Schaniel, Th. Woike, Phys. Chem. Chem. Phys. 11 (2009) 4391.

[3] J.H. Enemark, R.D. Feltham, Coordn. Chem. Rev. 13 (1974) 339.

[4] *Materials*: RuCl$_3$·xH$_2$O was used as supplied by Sigma–Aldrich. Pyrazole-3,5-dicarboxylic acid monohydrate, KNO$_2$, HCl (37%) and potassium hydroxide were purchased from Fluka and used without further purification. Ethanol, methanol, diethyl ether and 1 m KOH were used as supplied by Merck. K$_2$[Ru(NO)Cl$_5$] was prepared according to a literature procedure (J.R. Durig, W.A. McAllister, J.N. Willis, E.E. Mercer, Spectrochim. Acta 22 (1966) 1091–1100). The described compounds are stable in air. *NMR spectroscopy*: NMR spectra were recorded at room temperature on a Jeol Eclipse 400 (^{1}H: 400 MHz, ^{13}C{^{1}H}: 101 MHz) NMR spectrometer. The signals of the deuterated solvent (^{13}C{^{1}H}) and the residual protons therein (^{1}H) were used as an internal secondary reference for the chemical shift. For atom numbering see Fig. 1. *Mass spectrometry*: Mass spectra were measured on a Thermo Finnigan LTQ FT with IonMax (ion source with ESI head). *UV–vis and IR spectroscopy*: UV–vis: Varian Cary 50 Bio (10-mm quartz-glass cuvettes); IR: Jasco FT/IR-460plus equipped with a single-reflection ATR diamond plate (solid samples). *Crystal-structure determination and refinement*: A suitable crystal was selected with the aid of a polarisation microscope, mounted on the tip of a glass fibre and investigated at 200 K on a Nonius Kappa CCD diffractometer with graphite-monochromated Mo Kα radiation (λ = 0.71073 Å). The structure was solved by direct methods (SIR97) and refined by full-matrix least-squares calculations on F^2 (SHELXL-97). Anisotropic displacement parameters were refined for all non-hydrogen atoms.

[5] *Preparation of 1*: K$_2$[Ru(NO)Cl$_5$] (329 mg, 0.851 mmol) was suspended in 100 mL ethanol–H$_2$O (3:1), then pyrazole-3,5-dicarboxylic acid monohydrate (148 mg, 0.850 mmol), dissolved in 3 mL ethanol–H$_2$O (3:1), was added dropwise to the suspension. The pH value of the suspension was adjusted to 8 with 1 m KOH, and the mixture was refluxed for 1 h. The resulting solution was evaporated to dryness on a rotary evaporator and the residue suspended in 15 mL methanol. After addition of 5 mL of H$_2$O, the orange-brown suspension was left standing at room temperature for 24 h. The solid was collected by filtration, washed with 30 mL methanol, 10 mL ice-cold water and 50 mL diethyl ether and vacuum-dried. **1** was obtained as a yellow powder of the composition **1** + 1.5 H$_2$O (77.0 mg, 0.103 mmol, 24.3% yield). ^{1}H NMR (399.78 MHz, d$_6$-DMSO, 23 °C) δ/ppm: 6.93 (s, 2H, H3). ^{13}C{^{1}H} NMR (100.53 MHz, d$_6$-DMSO, 25 °C) δ/ppm: 167.66 (C1+C5), 146.44 (C2+C4), 104.79 (C3). UV-vis (DMSO): λ_{max}/nm (ε/mol^{-1} dm^3 cm^{-1}): 310 (sh.) (6093), 394 (sh.) (429), 468 (sh.) (186). IR: ν_{max}/cm^{-1}: 3565 (w), 3502 (w), 3468 (w), 3434 (w), 3124 (w), 1892 (vs), 1645 (vs), 1597 (m), 1558 (w), 1506 (vw), 1480 (m), 1409 (vw), 1386 (m), 1346 (s), 1239 (s), 1207 (vs), 1103 (w), 1077 (w), 1025 (vs), 853 (m), 842 (m), 807 (w), 774 (vs), 715 (vw), 709 (vw), 701 (vw), 685 (vw), 676 (vw), 671 (vw), 663 (vw), 658 (vw), 652 (vw), 646 (w), 637 (w), 623 (m), 610 (m), 604 (m). MS-ESI (positive ions, M = C$_{10}$H$_2$Cl$_2$K$_2$N$_6$O$_{10}$Ru$_2$ = **1**) m/z: 680.7092 (Ru$_2$ pattern, [M+2H–K]$^+$, calc. 680.7082), 718.6650 (Ru$_2$ pattern, [M+H]$^+$, calc. 718.6641), 755.6216 (Ru$_2$ pattern, [M+K]$^+$, calc. 758.6195). MS-ESI (negative ions, M = C$_{10}$H$_2$Cl$_2$K$_2$N$_6$O$_{10}$Ru$_2$ = **1**) m/z: 640.7368 (Ru$_2$ pattern, [M+H–2K]$^-$, calc. 640.7379), 677.6932 (Ru$_2$ pattern, [M–K]$^-$, calc. 678.6937). Elemental analysis (%) calc. for C$_{10}$H$_5$Cl$_2$K$_2$N$_6$O$_{11.5}$Ru$_2$ (**1** + 1.5 H$_2$O, 744.43 g mol^{-1}) (the existence of 1.5 equiv. of H$_2$O in the amorphous compound was confirmed by thermogravimetric measurements showing a mass decrease of 3.83% in the temperature range of 25–150 °C, which is in agreement with the expected value of 3.63%) C 16.13, H 0.68, Cl 9.52, N 11.29. Found: C 16.28, H 0.99, Cl 9.28, N 11.53.

[6] *Preparation of 2*: K$_2$[Ru(NO)Cl$_5$] (787 mg, 2.04 mmol) was suspended in 100 mL ethanol–H$_2$O (3:1), then pyrazole-3,5-dicarboxylic acid monohydrate (354 mg, 2.03 mmol), dissolved in 6 mL ethanol–H$_2$O (3:1), was added dropwise to the suspension. The pH value of the suspension was adjusted to 8 with 1 m KOH, and the mixture was refluxed for 1 h. The resulting suspension was filtered and the filter cake was suspended in 60 mL H$_2$O, refluxed for 3 h and filtered again. The microcrystalline solid was washed with 100 mL H$_2$O and 50 mL diethyl ether and vacuum-dried. The product was obtained as a yellow, anhydrous powder of the composition **2** – 2 H$_2$O (153 mg, 0.239 mmol, 23.5% yield). Crystals of **2** formed in a saturated solution of **1** in H$_2$O–methanol (4:1) by slow evaporation of the solvent at room temperature. ^{1}H NMR (399.78 MHz, d$_6$-DMSO, 22 °C) δ/ppm: 10.61 (br s, 4H, 2H$_2$O), 7.14 (s, 2H, H3). ^{13}C{^{1}H} NMR (100.53 MHz, d$_6$-DMSO, 23 °C) δ/ppm: 167.44 (C1+C5), 147.24 (C2+C4), 105.68 (C3). UV-vis (DMF): λ_{max}/nm (ε/mol^{-1} dm^3 cm^{-1}): 284 (sh.) (12395), 378 (sh.) (745), 465 (sh.) (238). IR: ν_{max}/cm^{-1}: 3505 (w), 3400 (w), 3129 (m), 1916 (vs), 1619 (vs), 1602 (vs), 1587 (vs), 1575 (vs), 1558 (vs), 1485 (s), 1473 (m), 1392 (m), 1368 (w), 1345 (vs), 1286 (w), 1264 (vs), 1240 (vs), 1131 (m), 1124 (m), 1090 (m), 1026 (s), 907 (m), 857 (s), 797 (w), 780 (vs), 695 (vw), 685 (vw), 678 (vw), 668 (vw), 659 (w), 651 (m), 639 (vw), 627 (m), 614 (m). MS-ESI (negative ions, M = C$_{10}$H$_6$N$_6$O$_{12}$Ru$_2$ = **2** – 4 H$_2$O) m/z: 603.8073 (Ru$_2$ pattern, [M–H]$^-$, calc. 603.8077). Elemental analysis (%) calc. for C$_{10}$H$_{10}$N$_6$O$_{14}$Ru$_2$ (**2** – 2 H$_2$O, 640.36 g mol^{-1}) (the existence of 4 equiv. of H$_2$O in the microcrystalline compound was confirmed by thermogravimetric measurements showing a mass decrease of 12.1% in the temperature range of 25–150 °C, which is in agreement with the expected value of 11.3%) C 18.76, H 1.57, Cl 0.00, N 13.12. Found: C 18.64, H 1.38, Cl 0.00, N 13.07.

[7] Crystallographic data of [{Ru(NO)(H$_2$O)}$_2$(μ-pzdc)$_2$]·4H$_2$O (**2**): C$_{10}$H$_{14}$N$_6$O$_{16}$Ru$_2$, M_r = 676.41 g mol^{-1}, crystal size: 0.15 × 0.10 × 0.09 mm, T = 200(2) K, triclinic, $P\bar{1}$, a = 7.8919(3), b = 8.2076(2), c = 9.6122(3) Å, α = 66.611(2), β = 70.856(2), γ = 62.587(2)°, V = 499.17(3) Å^3, Z = 1, ρ = 2.250 g cm^{-3}, μ = 1.611 mm^{-1}, absorption correction: multi-scan (SADABS, version 2, G.M. Sheldrick, University of Göttingen, 2001), T_{min}/T_{max} = 0.723, 8486 reflections, R_{int} = 0.0233, mean $\sigma(I)/I$ = 0.0257, θ range = 3.17–27.5°, 2135 observed reflections, 2257 reflections in refinement, x, y (weighting scheme): 0.0147 and 1.0518, 174 parameters, 9 restraints, $R(F_{obs})$ = 0.0233, $R_w(F^2)$ = 0.0551, S = 1.094, shift/error$_{max}$ = 0.001, max. and min. residual density: 0.687 and –0.731 eÅ^{-3}.

[8] D. Cremer, J.A. Pople, J. Am. Chem. Soc. 97 (1975) 1354.

[9] (a) J.A. Güida, M.A. Ramos, O.E. Piro, P.J. Aymonino, J. Mol. Struct. 609 (2002) 39;

(b) A. Zangl, P. Klüfers, D. Schaniel, Th. Woike, J. Chem. Soc., Dalton Trans. (2009) 1034.

[10] *Low-temperature infrared spectroscopy and PLI measurements*: The infrared spectra were detected with a Nicolet 5700 FTIR spectrometer. The fine powder of samples **1** and **2** was mixed with KBr and pressed to a pellet. The KBr pellet was mounted on a copper cold finger using silver paste for good thermal contact. The sample was cooled to 85 K in a liquid nitrogen cryostat. KBr windows allowed the irradiation of the sample with laser light and absorption measurements down to 390 cm^{-1}. The irradiation was performed by the monochromatic light of an argon laser at 457.9 nm, 476.5 nm, 488 nm, 496.5 nm, or 514 nm or a HeCd laser at 442 nm for the population of the metastable state MS1. The transfer from MS1 into MS2 was performed with light of a Nd:YAG laser at 1064 nm after MS1 had been previously generated up to saturation with blue–green light. Depopulation of MS1 and/or MS2 was performed with 660 nm from a diode laser.

[11] Th. Woike, W. Krasser, H. Zöllner, W. Kirchner, S. Haussühl, Z. Phys. D 25 (1993) 351.

[12] A. Schuy, Th. Woike, D. Schaniel, J. Sol–Gel Sci. Technol. 50 (2009) 403.